ISSN 2075-1133, Inorganic Materials: Applied Research, 2018, Vol. 9, No. 5, pp. 900–905. © Pleiades Publishing, Ltd., 2018.
Original Russian Text © A.A. Lukin, N.B. Kolchugina, Yu.S. Koshkid'ko, A.V. Kamynin, D.Yu. Vasilenko, 2018, published in Perspektivnye Materialy, 2018, No. 3, pp. 19–27.

GENERAL-PURPOSE MATERIALS

Magnetic Properties of the $Sm(Co_{0.45}Fe_{0.15}Cu_{0.40})_5$ Alloy Prepared by Strip Casting

A. A. Lukin[a, *], N. B. Kolchugina[b, **], Yu. S. Koshkid'ko[c, *], A. V. Kamynin[a], and D. Yu. Vasilenko[d]**

[a] *JSC Spetsmagnit, Moscow, 127238 Russia*
[b] *Baikov Institute of Metallurgy and Materials Science, Russian Academy of Sciences, Moscow, 119334 Russia*
[c] *Institute of Low Temperature and Structure Research, Polish Academy of Sciences, Wroclaw, 50-422 Poland*
[d] *Ural Electomechanical Plant, Yekaterinburg, 620137 Russia*
**e-mail: lukinaalukin@rambler.ru*
***e-mail: natalik@imet.ac.ru*
****e-mail: yurec@mail.ru*

Received October 23, 2017

Abstract—The magnetic properties and phase composition of the $Sm(Co_{0.45}Fe_{0.15}Cu_{0.40})_5$ alloy prepared by the strip-casting technique (the casting of alloy on a water-cooled copper wheel at a velocity of cooling surface of ~1 m/s) are studied. Curves of magnetization of thermally demagnetized starting plates (after strip casting) and plates subjected to low-temperature treatment at 350°C for 120 h and the hysteresis loops were measured in magnetizing fields of up to 140 kOe. It is shown that the magnetization of samples (σ^{140} and σ_r) substantially decreases after the annealing; in this case, the coercive force ($_jH_c$) increases abruptly. It is assumed that the observed regularities of magnetic hardening can be related to the existence of nanosized Cu-enriched areas, within which the antiferromagnetic order in the $Sm(Co, Fe, Cu)_5$ lattice is realized. These areas in the ferromagnetic phase with the lower copper content can be domain-wall pinning centers.

Keywords: $Sm(Co_{0.45}Fe_{0.15}Cu_{0.40})_5$ alloy, strip casting, structure, magnetic properties, hysteretic characteristics, antiferromagnetic order

DOI: 10.1134/S2075113318050192

INTRODUCTION

To date, a good many works related to the investigation of magnetic properties and structure of sintered $Sm(Co, Fe, Cu, Zr)_{7–8}$-based magnets were performed. It was shown that the high-coercivity state of these magnets is realized in the presence of a nanoheterogeneous structure consisting of rhomb-shaped $Sm_2(Co, Fe)_{17}$-phase cells (with the Th_2Zn_{17}-type structure) 70–100 nm in size; the $Sm(Co, Fe, Cu)_5$ phase (with the $CaCu_5$-type structure) is located at boundaries of $Sm_2(Co, Fe)_{17}$-phase cells. The structure of magnets also includes Z-phase plates arranged perpendicular to the magnetic texture axis. The Z-phase composition is $(Sm, Zr)(Co, Fe)_3$ (with the Be_3Nb-type structure) or $(Sm, Zr)_2(Co, Fe)_7$ (with the Ce_2Ni_7-type structure). It was found that an abrupt increase in the magnetization coercive force ($_jH_c$) from 1–2 to 20–40 kOe [1–10] is observed after prolonged cooling (for more than 4 h) from 780–850 to 400°C, during which the diffusion of copper within the grain-boundary 1-5 phase, namely, from cell boundaries into the grain-boundary phase, occurs [1–10]. According to the majority of these studies, the high values of the coercive force $_jH_c$ are explained by the realization of domain-wall (DW) pinning at the boundary between $Sm_2(Co, Fe)_{17}$ and $Sm(Co, Fe, Cu)_5$ phases, which are characterized by different values of the boundary-energy density [1, 2, 5–10]. In particular, in situ transmission electron-microscopic observations of the domain structure during magnetization reversal [11] showed that zigzag DWs are located along the boundary $Sm(Co, Fe, Cu)_5$ phase. Some investigators explain the high-coercivity state of $Sm(Co, Fe, Cu, Zr)_{7–8}$ magnets by either peculiarities of magnetization reversal of small particles [12] or a mixed mechanism of magnetization reversal (DW pinning along with the irreversible magnetization rotation within the cell phase in different areas of magnet) [13]. According to data of [14], the DW pinning is realized at the contact of $Sm(Co, Fe, Cu)_5$- and Z-phase plates. However, a number of observed peculiarities of coercive force variations cannot be explained in terms of the aforementioned approaches. One of the peculiarities is the substantial violation of the dependence of coercive force $_jH_c$ on the angle of the applied field during magnetization reversal, namely, the decrease in the coercive force in the presence of a transverse com-

ponent of the applied field, which is observed for $Sm(Co, Fe, Cu, Zr)_{7-8}$ materials [15]. This leads to the deviation of angular dependence of ${}_jH_c$ from the dependence calculated for the traditional mechanism of magnetization reversal, which is due to the DW pinning within areas characterized by the lower values of boundary energy [15].

In the case of this mechanism of magnetization reversal, the ${}_jH_c$ coercive force is determined only by the normal component of the applied magnetic field, i.e., by the field applied along the easy magnetization axis or texture axis. When the applied field makes an angle with the easy magnetization axis, the magnetization reversal is realized only with the normal component of the applied field; in this case, the transverse component of the magnetic field does not affect the magnetization reversal process. Because of this, during magnetization reversal with a field applied at an angle to the easy magnetization axis, the ${}_jH_c$ magnitude increases and, as the angle increases, demonstrates an angular dependence characterized by a maximum (corresponding to a certain angle) and a subsequent rather abrupt decrease in the coercive force almost to zero.

One more peculiarity, which cannot be explained in terms of the traditional mechanism of magnetization reversal due to the DW pinning, is the monotonic increase in ${}_jH_c$ after cooling from 780–850 to 400°C in the course of low-temperature treatment (LTT) [12].

The ambiguity in understanding the mechanism of magnetization reversal makes difficult the choice of optimum technological conditions used in manufacturing magnets and prediction of variations of properties of magnets during their operation.

To clarify the mechanism of magnetization reversal of $Sm(Co, Fe, Cu, Zr)_{7-8}$ magnets, attempts to study properties of one of the individual structural components, namely, the boundary $Sm(Co, Fe, Cu)_5$ phase, were made. Its microstructure and local chemical composition, which was determined with a resolution of several nanometers, etc., were studied in conjunction with the magnetic properties and LTT conditions, and regularities common for $Sm(Co, Fe, Cu, Zr)_{7-8}$ magnets and individual $Sm(Co, Fe, Cu)_5$ phase were found. The temperature of the final stage of LTT (350–400°C), coercive force magnitude ${}_jH_c$, identified nanoheterogeneity (at a level of several nanometers), and behavior of the magnetization curve from the thermally demagnetized state [16, 17] are among the regularities.

In the present study, the magnetic properties and structure of the $Sm(Co_{0.45}Fe_{0.15}Cu_{0.40})_5$ alloy prepared by the strip-casting technique are investigated. Previously, only powder samples textured in a magnetic field were studied [16].

The aim of the present study is to analyze the mechanism of magnetization reversal of the $Sm(Co_{0.45}Fe_{0.15}Cu_{0.40})_5$ alloy prepared by the strip-casting technique and to compare the results with data available for processes of magnetization reversal for $Sm(Co, Fe, Cu, Zr)_{7-8}$ alloys and sintered magnets; the analysis is performed using the results of magnetic measurements and X-ray diffraction studies.

EXPERIMENTAL

The $Sm(Co_{0.45}Fe_{0.15}Cu_{0.40})_5$ alloy plates 340–360 μm thick were prepared by the strip-casting technique (melt casting on a water-cooled copper wheel; the velocity of the cooling surface was ~1 m/s). The alloy composition was determined by microwave plasma atomic emission spectroscopy using a Spectro-Sky-002 spectrometer. Sintered magnets were prepared by the standard technology, which includes the following processes: milling of alloy plates, compacting of powder preliminarily textured in a magnetic field, sintering of compacts in a vacuum at 1150°C, thermal and mechanical treatments of magnets, and their magnetization. The alloy plates were subjected to low-temperature treatment (LTT), namely, holding in a high-purity argon atmosphere at 350°C for 120 h followed by quenching. In this case, after LTT, almost a half of the plates became "bright pink" in color (from here on, "bright" plates); the other plates became slightly dark ("dark" plates). The chemical analysis of the plates subjected to LTT showed that the copper content in "bright" plates was ~1 wt % higher than that in "dark" plates.

X-ray diffraction analysis of powders prepared from starting and heat-treated plates (patterns were taken from the plate surface) and sintered magnets (patterns were taken from pole surfaces) was performed using a DRON-3M diffractometer with CuK_α radiation and a graphite monochromator.

According to the orientation of plates in a uniform magnetic field of 15 kOe, their easy magnetization axis (EMA) makes an angle of ~45° with the plate surface; i.e., when the magnetic field is applied along the long axis of plate and perpendicular to the plate surface, the EMA of plate makes an angle of ~45° with the applied magnetic field direction.

The magnetic properties of magnets (in measuring the hysteresis loops) were studied at room temperature in magnetic fields of up to 140 kOe using equipment available in the International Laboratory of High Magnetic Fields and Low Temperatures, Polish Academy of Sciences (Wroclaw, Poland), namely, using an Oxford superconducting magnet and an original vibrating-sample magnetometer.

The magnetic properties of magnets at room temperature were measured in magnetic fields of up to 12 MA/m using a closed magnetic circuit and a MH-50 hysteresisgraph. Samples of magnets were preliminarily magnetized in pulsed magnetic fields of up to 140 kOe.

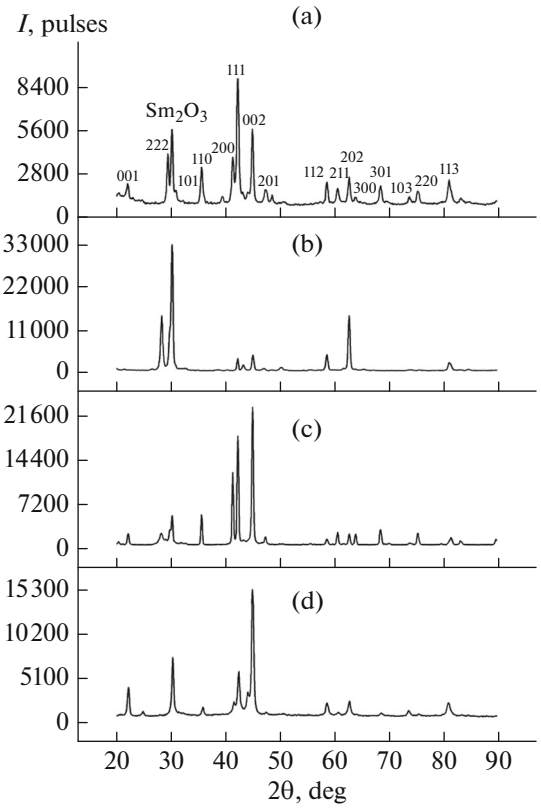

Fig. 1. X-ray diffraction patterns for the $Sm(Co_{0.45}Fe_{0.15}Cu_{0.40})_5$ alloy: (a) powder samples prepared from starting "strip-casting" plates, (b) free and (c) contact surfaces of the plates, and (d) pole surfaces of sintered magnet.

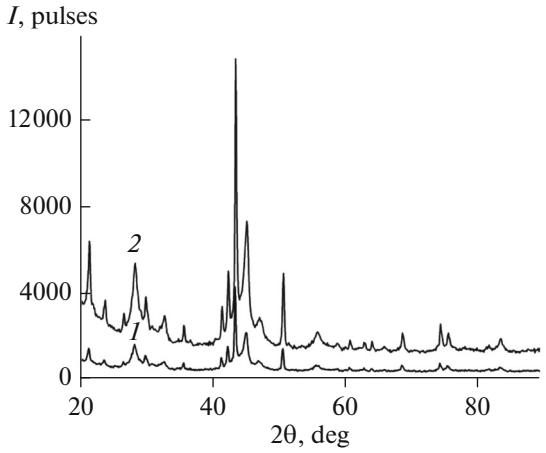

Fig. 2. X-ray diffraction patterns taken for the $Sm(Co_{0.45}Fe_{0.15}Cu_{0.40})_5$ "bright" plates subjected to LTT at 350°C for 120 h; exposure: (*1*) 3 and (*2*) 15 s.

RESULTS AND DISCUSSION

Figure 1 shows X-ray diffraction (XRD) patterns for the $Sm(Co_{0.45}Fe_{0.15}Cu_{0.40})_5$ alloy taken for (a) isotropic powders prepared from starting plates, (b) free and (c) contact (contacting the copper wheel) surfaces of plates, and (d) pole surfaces of sintered magnets. Despite of the fact that the XRD pattern taken for the isotropic powder differs from those taken for the free and contact surfaces of plates (Figs. 1b, 1c) and sintered magnets, all the reflections (except the reflection observed at $2\theta = \sim 30°$, which corresponds to samarium oxide) in the XRD patterns are indexed as belonging to the $Sm(Co, Cu, Fe)_5$ compound with the $CaCu_5$-type structure.

Figure 2 shows XRD patterns taken (for expositions of 3 and 15 s) for "bright" $Sm(Co_{0.45}Fe_{0.15}Cu_{0.40})_5$ plates subjected to LLT. An analysis of the XRD patterns exhibits the presence of a phase (reflections corresponding to $2\theta = \sim 51°$) with the Cu-type structure (space group $Fm\bar{3}m$). The formation of Cu-rich segregations were observed for oxidized $Sm(Co, Fe, Cu, Zr)_z$ magnets in [18]. In our case, since the probability of surface oxidation of plates during LTT cannot be excluded, the appearance of Cu segregation on the surface of plates is fully explainable. After etching the surface layer of "bright" plates, the XRD patterns of "bright" and "dark" plates become identical.

Curves of magnetization of thermally demagnetized starting (after strip-casting) and heat-treated ("dark" and "bright") plates were measured in magnetizing fields of up to 140 kOe, which were applied in the plane of the plate along the direction of motion of the quenching wheel (longitudinal direction) and perpendicular to the plate surface (perpendicular direction). Results of the measurements are given in Fig. 3 and Table 1.

According to data given in Table 1, the LTT leads to a substantial decrease in the magnetization in a field of 140 kOe (σ^{140}) and residual magnetization (σ_r). In this case, the coercive force ${}_jH_c$ abruptly increases. The "necking" in the magnetization-reversal portion of hysteresis loop of "bright" plates (Fig. 3) is likely related to the presence of surface Cu segregations. The behavior of the hysteresis loop changes (the "necking" disappears) after etching the surface layer.

The decrease in the residual magnetization and simultaneous increase in the magnetization coercive force were observed also for sintered magnets prepared from this alloy. The analogous regularities (the 2-fold decrease in the residual magnetization and 4-fold increase in ${}_jH_c$) were observed in [16] in studying textured powders of the analogous alloy subjected to homogenizing annealing at 1050°C and LTT at 400°C. In this case, no additional phases such as $Sm_2(Co, Fe)_{17}$ and $SmCo_3$ were found, the presence of which in sintered $Sm(Co, Fe, Cu, Zr)_{7-8}$ magnets explains their high (30–40 kOe) values of ${}_jH_c$. High-resolution data of transmission electron microscopy obtained for $Sm(Co_{0.45}Fe_{0.15}Cu_{0.40})_5$ alloy in [17] indicate only the existence of a slight contrast for areas several nanome-

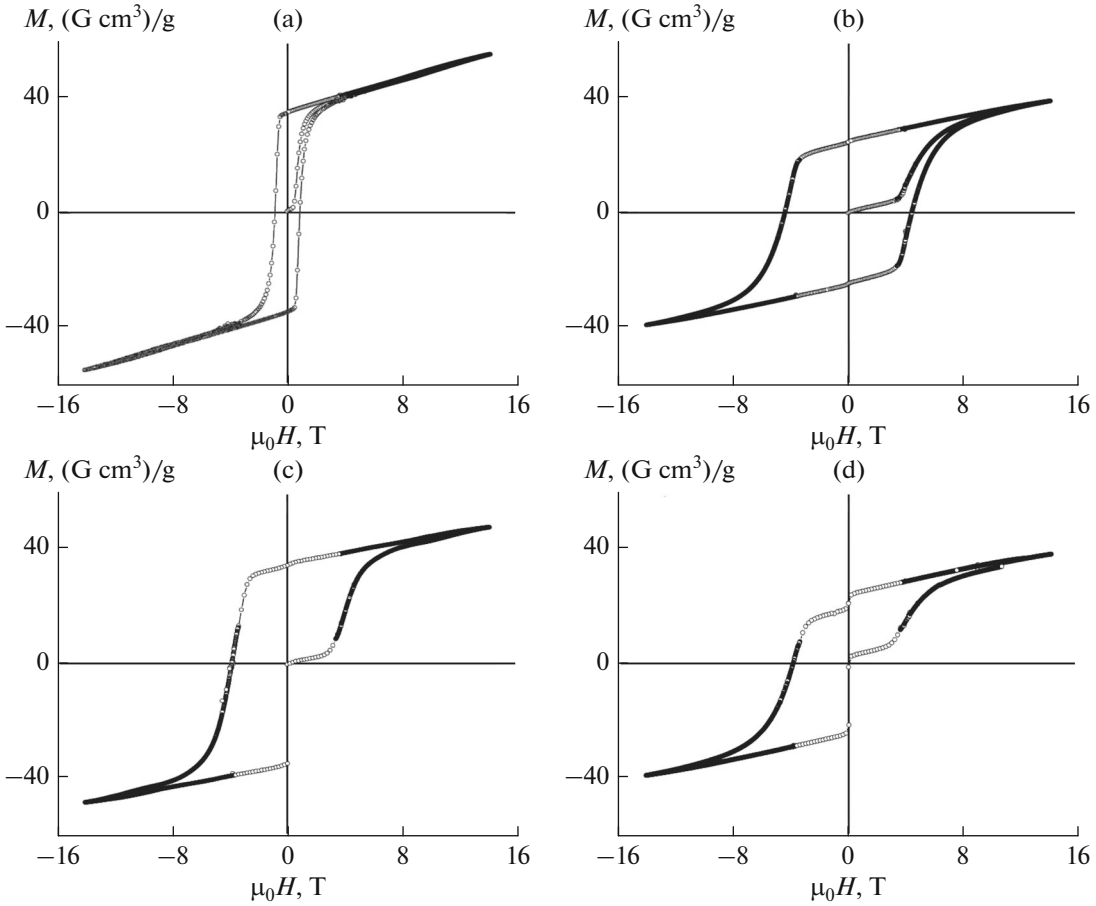

Fig. 3. Magnetization curves and hysteresis loops measured at room temperature: (a) starting strip-casting $Sm(Co, Cu, Fe)_5$ alloy; (b, c) "dark" plate subjected to LTT at 350°C for 120 h; and (d) "bright" plate subjected to LTT at 350°C for 120 h. Magnetizing field is applied (a, b, d) in plate surface along the quenching surface motion direction and (c) perpendicular to the plate surface.

ters in size. This fact does not allow us to relate the high ${}_jH_c$ values to the chemical composition gradient of the ferromagnetic component or to consider these nano-heterogeneities as DW pinning centers (since a marked difference between values of boundary-energy density is absent).

In our opinion, the observed regularities (the decrease in the magnetization and abrupt increase in the magnetization coercive force) can be explained by peculiarities of the $CaCu_5$-type structure, which are responsible for the magnetic behavior of considered alloys. As the copper content within some nanosized areas increases (by means of LTT-induced separation), copper atoms mainly are located in the Sm-atom layer and, thus, the following sequence of layers forms: Sm + Cu–Co + Fe–Sm + Cu–Co + Fe; the

Table 1. Magnetic characteristics of the $Sm(Co_{0.45}Fe_{0.15}Cu_{0.40})_5$ alloy

State		Magnetizing field direction	Magnetization in a field of 140 kOe σ^{140}, (G cm^3)/g	Residual magnetization σ_r, (G cm^3)/g	Magnetization coercive force ${}_jH_c$, kOe	Hysteresis-loop squareness parameter H_k, kOe
Initial		Longitudinal	55.0	35.0	7.0	5.0
LTT at 350°C for 120 h, quenching	"Dark" plate	Longitudinal	40.0	24.5	44.4	19.0
		Perpendicular	47.4	33.3	38.0	27.0
	"Bright" plate	Longitudinal	38.6	20.3	34.2	18.1

layers are perpendicular to the *C* axis (magnet texture axis coinciding with the *c* crystallographic axes of individual grains). In this case, the layers in the $Sm(Co, Fe, Cu)_5$ lattice are antiferromagnetically coupled, and the high coercive force is due to the pinning of DWs of the ferromagnetic phase at antiferromagnetic nanoareas enriched in copper (which are DW pinning centers).

This fact is indicated by data of [19]. According to the data, in $SmCo_3Cu_2$ alloys, the ordering of copper and cobalt atoms in the $SmCo_5$ lattice is observed after LTT at 400°C; in this case, copper atoms are located within Sm layers, whereas cobalt atoms are present in parallel alternating planes. Such a structure is typical of antiferromagnets, in which the indirect exchange coupling between ferromagnetic (cobalt) layers is realized with conduction electrons [20].

The approach suggested in the present study allows us to explain the decrease in the magnetization of samples (by the formation of antiferromagnetic areas characterized by lower magnetization) and to attempt to explain the atypical dependence of ${}_jH_c$ on the angle of applying the magnetic field (the decrease in the coercivity of material in the presence of the perpendicular component of magnetization-reversing magnetic field) by the metamagnetic transition (from the antiferromagnetic to ferromagnetic state) in lower fields in the presence of the perpendicular component of the magnetic field. The monotonic increase in ${}_jH_c$ of sintered $Sm(Co, Fe, Cu, Zr)_{7-8}$ magnets after slow cooling from 780–830 to 350–400°C is related to the copper separation and ordering of copper and cobalt atoms in the 1-5 phase lattice.

Thus, in sintered $Sm(Co, Fe, Cu, Zr)_{7-8}$ magnets, the $Sm(Co, Fe, Cu)_5$ cell-boundary phase forms the high coercivity of magnets, whereas the role of the $Sm_2(Co, Fe)_{17}$ phase consists in the substantial increase in the saturation magnetization and maximum energy product of sintered magnets. Additional requirements which are imposed on the $Sm_2(Co, Fe)_{17}$ phase in $Sm(Co, Fe, Cu, Zr)_{7-8}$ magnets are the high magnetic anisotropy field (H_a), the value of which should be higher than the coercive force due to the DW pinning (H_a = 80–100 kOe > ${}_jH_c$ = 20–40 kOe), and cell sizes (80–120 nm) of less than the single-domain size (~300 nm). These requirements limit the possibility for the increase in the maximum energy product because of the need to have a sufficient amount of the $Sm(Co, Fe, Cu)_5$ phase (characterized by the lower magnetization) in the magnet composition. In this case, the iron content in the $Sm_2(Co, Fe)_{17}$ phase should be limited since the increase in the iron content leads to the substantial decrease in the anisotropy field (H_a). Usually, alloys with no more than 15–17 wt % Fe are used. For some perfect samples, the iron content can be increased to 25 wt % [21]; however, this makes the technology substantially more complex (since it assumes both low-oxygen manufacturing processes and significant increase in the time of homogenizing annealing and LTT).

CONCLUSIONS

The performed analysis of the magnetic properties of the $Sm(Co_{0.45}Fe_{0.15}Cu_{0.40})_5$ alloy prepared by the strip-casting technique and subjected to prolonged low-temperature treatment allows us to draw an analogy between the magnetization reversal mechanisms for the $Sm(Co, Fe, Cu)_5$ and $Sm(Co, Fe, Cu, Zr)_{7-8}$ alloys.

In both cases, namely, in the cases of the antiferromagnetic (the higher ${}_jH_c$ values observed after LTT) and ferromagnetic (in particular, the existence of coercive force for the starting strip-casting alloy) states, the mechanism of DW pinning at Cu-enriched areas within the $Sm(Co, Fe, Cu)_5$ phase is realized. The cellular $Sm_2(Co, Fe)_{17}$ phase in sintered $Sm(Co, Fe, Cu, Zr)_{7-8}$ magnets is a high-anisotropy ferromagnetic "filler" with a high saturation magnetization.

REFERENCES

1. Hadjipanayis, G.C., Tang, W., Zhang, Y., Chui, S.T., Liu, J. F., Chen, C., and Kronmüller, H., High temperature 2 : 17 magnets: Relationship of magnetic properties to microstructure and processing, *IEEE Trans. Magn.*, 2000, vol. 36, no. 5, pp. 3382–3387.
2. Gopalan, R., Hono, K., Yan, A., and Gutfleisch, O., Direct evidence for Cu concentration variation and its correlation to coercivity in $Sm(Co_{0.74}\text{-}Fe_{0.1}Cu_{0.12}Zr_{0.04})_{7.4}$ ribbons, *Scr. Mater.*, 2009, vol. 60, pp. 764–767.
3. Liu, L., Liu, Z., Chen, R., Liu, X., Yan, A., Lee, D., and Li, W., Effect of strip casting on microstructure and magnetic properties of 2:17 type Sm–Co sintered magnets, *IEEE Trans. Magn.*, 2014, vol. 50, no. 1, p. 2101704.
4. Liu, Z., Liu, L., Chen, R.J., Sun, Y.L., Lee, D., and Yan, A.R., Optimization of temperature coefficient of remanence and magnetic properties of sintered $Sm_{0.7}Dy_{0.1}Gd_{0.2}(Co_{bal}Fe_{0.2}Cu_{0.08}Zr_{0.025})_{7.2}$ magnets prepared by strip-casting technique, *IEEE Trans. Magn.*, 2013, vol. 49, no. 12, pp. 5599–5603.
5. Liu, L, Liu, Z., Zhang, X., Feng, Y., Wang, C., Sun, Y., Lee, D., Yan, A., and Wu, Q., Magnetization reversal process in $(Sm, Dy, Gd)(Co, Fe, Cu, Zr)_z$ magnets with different cellular structures, *AIP Adv.*, 2017, vol. 7, p. 056221.
6. Machida, H., Fujiwara, T., Kamada, R., Morimoto, Y., and Takezawa, M., The high squareness Sm–Co magnet having H_{cb} = 10.6 kOe at 150°C, *AIP Adv.*, 2017, vol. 7, p. 056223.
7. Nishida, Y., Endo, M., and Sakurada, S., A modeling study of domain wall pinning in Sm_2Co_{17}-based magnets, *J. Magn. Magn. Mater.*, 2012, vol. 324, pp. 1948–1953.
8. Sepehri-Amin, H., Thielsch, J., Fischbacher, J., Ohkubo, T., Schrefl, T., Gutfleisch, O., and Hono, K.,

Correlation of microchemistry of cell boundary phase and interface structure to the coercivity of $Sm(Co_{0.784}Fe_{0.100}Cu_{0.088}Zr_{0.028})_{7.19}$ sintered magnets, *Acta Mater.*, 2017, vol. 126, pp. 1–10.

9. Sun, W., Zhu, M., Guo, Z., Fang, Y., and Li, W., The coercivity mechanism of sintered $Sm(Co_{bal}Fe_{0.245}Cu_{0.07}Zr_{0.02})_{7.8}$ permanent magnets with different isothermal annealing time, *Phys. B* (Amsterdam), 2015, vol. 476, pp. 154–157.
10. Xiong, X.Y., Ohkubo, T., Koyama, T., Ohashi, K., Tawara, Y., and Hono, K., The microstructure of sintered $Sm(Co_{0.72}Fe_{0.20}Cu_{0.055}Zr_{0.025})_{7.5}$ permanent magnet studied by atom probe, *Acta Mater.*, 2004, vol. 52, pp. 737–748.
11. Tian, Y., Liu, Z., Xu, H., Du, J., Zhang, J., Xia, W., and Liu, J.P., In situ observation of domain wall pinning in $Sm(Co, Fe, Cu, Zr)_z$ magnet by Lorentz microscopy, *IEEE Trans. Magn.*, 2015, vol. 51, no. 11, p. 7114284.
12. Gutfleisch, O., Müller, K.-H., Khlopkov, K., Wolf, M., Yan, A., Schäfer, R., Gemming, T., and Schultz, L., Evolution of magnetic domain structures and coercivity in high-performance SmCo 2 : 17-type permanent magnets, *Acta Mater.*, 2006, vol. 54, pp. 997–1008.
13. Lyakhova, M.B., Semenova, E.M., Pastushenkov, Yu.G., Pastushenkov, A.G., Sinekop, V.I., and Zezyulina, P.A., Magnetic domain structure and magnetic reversal process of $(R, Zr)(Co, Cu, Fe)_z$ heterogeneous nanocrystalline alloys, *Solid State Phenom.*, 2011, vols. 168–169, pp. 400–403.
14. Duerrschnabel, M., Yi, M., Uestuener, K., Liesegang, M., Katter, M., Kleebe, H.-J., Xu, B., Gutfleisch, O., and Molina-Luna, L., Atomic structure and domain wall pinning in samarium-cobalt-based permanent magnets, *Nat. Commun.*, 2017, vol. 8, no. 54, pp. 1–7.
15. Suponev, N.P., Grechishkin, R.M., Lyakhova, M.B., and Pushkar, Yu.E., Angular dependence of coercive field in $(Sm, Zr)(Co, Cu, Fe)_z$, *J. Magn. Magn. Mater.*, 1996, vol. 157–158, pp. 376–377.
16. Zhang, Y., Gabay, A.M., and Hadjipanayis, G.C., Observation of the lamellar phase a Zr-free $Sm(Co_{0.45}Fe_{0.15}Cu_{0.40})_5$, *Appl. Phys. Lett.*, 2005, vol. 87, p. 141910.
17. Gabay, A.M., Larson, P., Mazin, I.I., and Hadjipanayis, G.C., Magnetic states and structural transformations in $Sm(Co, Cu)_5$ and $Sm(Co, Fe, Cu)_5$ permanent magnets, *J. Phys. D: Appl. Phys.*, 2005, vol. 38, pp. 1337–1341.
18. Pragnell, W.M., Williams, A.J., and Evans, H.E., The oxidation of SmCo magnets, *J. Appl. Phys.*, 2008, vol. 103, p. 07E127.
19. Katsikini, M., Pinakidou, F., Paloura, E. C., Gabay, A.M., and Hadjipanayis, G.C., Effect of aging on the nanostructure of $SmCo_3Cu_2$ magnets: An EXAFS study, *Proc. XXIV Pan-Hellenic Conf. on Solid State Physics and Materials Science*, Heraklion, 2008, p. 211.
20. Belov, K.P., Levitin, R.Z., and Nikitin, S.A., Ferro- and anti-ferromagnetism of rare earth metals, *Usp. Fiz. Nauk*, 1964, vol. 82, pp. 449–498.
21. Horiuchi, Y., Hagiwara, M., Endo, M., Sanada, N., and Sakurada, S., Influence of intermediate-heat treatment on the structure and magnetic properties of iron-rich $Sm(CoFeCuZr)_z$ sintered magnets, *J. Appl. Phys.*, 2015, vol. 117, art. ID 17C704.

Translated by N. Kolchugina